Inorg. Chem. **2005**, *44*, 4586–4593

Synthesis and Characterization of the Face-Sharing Bioctahedral $[Mo_2O_6F_3]^{3-}$ Anion

Janet E. Kirsch, Heather K. Izumi, Charlotte L. Stern, and Kenneth R. Poeppelmeier*

Department of Chemistry, Northwestern University, Evanston, Illinois 60208-3113

Received February 23, 2005

The face-sharing bioctahedral molybdenum(VI) oxide fluoride anion $[Mo_2O_6F_3]^{3-}$ has been isolated in the new compound $[Cu(3\text{-apy})_4]_3(Mo_2O_6F_3)_2$ (3-apy = 3-aminopyridine) and has been characterized by experimental and computational techniques. Single-crystal X-ray diffraction studies show that the structure of the $[Mo_2O_6F_3]^{3-}$ anion resembles two distorted face-sharing octahedra, each with three short terminal metal–ligand bonds and three long metal–ligand–metal bridging interactions. Aspects of the electronic structure, as well as geometric comparisons of the bond lengths and angles in $[Mo_2O_6F_3]^{3-}$ with those in the similarly distorted $[MoO_3F_3]^{3-}$ anion, suggest that the six terminal ligand positions of the confacial bioctahedra are occupied exclusively by oxide ligands and that the three bridging sites are occupied by fluorides. Crystal data for $[Cu(3\text{-apy})_4]_3(Mo_2O_6F_3)_2$: trigonal space group $R\bar{3}$ (No. 148) with hexagonal axes of $a = 13.881(1)$ Å and $c = 31.783(3)$ Å ($Z = 3$).

Introduction

Out-of-center octahedral distortions are responsible for the strong nonlinear optical responses exhibited by $LiNbO_3$[1] and $KTiOPO_4$,[2] two landmark solid state mixed-metal oxides. Similar distorted octahedral geometries are observed in early d^0 transition metal oxide fluoride anions. In these species, which have the general formula $[MO_xF_{6-x}]^{2-}$ ($x = 1$, M = V^{5+}, Nb^{5+}, Ta^{5+}; $x = 2$, M = Mo^{6+}, W^{6+}), the central metal cation distorts toward the corner ($x = 1$) or edge ($x = 2$) of the octahedron that is occupied by the oxide ligand(s), as shown in Figure 1, structures a and b. These electronic or "primary" distortions of the oxide fluoride anions arise from $d\pi-p\pi$ metal−oxide orbital interactions[3] and are respectively referred to as C_4 or C_2 distortions, as they approximately coincide with the local C_4 or C_2 rotational axis of the anion. Short M═O bonds, long M−F bonds trans to the oxides, and bond angles that deviate from 90° are characteristic of these out-of-center distortions.

Another related oxyfluoro species is $[MoO_3F_3]^{3-}$ ($x = 3$). The $[MoO_3F_3]^{3-}$ octahedral unit has been reported previously in $(Ag_3MoO_3F_3)(Ag_3MoO_4)Cl$,[4] with the three oxide ligands located in a fac arrangement (see Figure 1c). This configuration allows for a more evenly distributed sharing of the metal d orbitals with the oxygen p orbitals.[5] In congruence

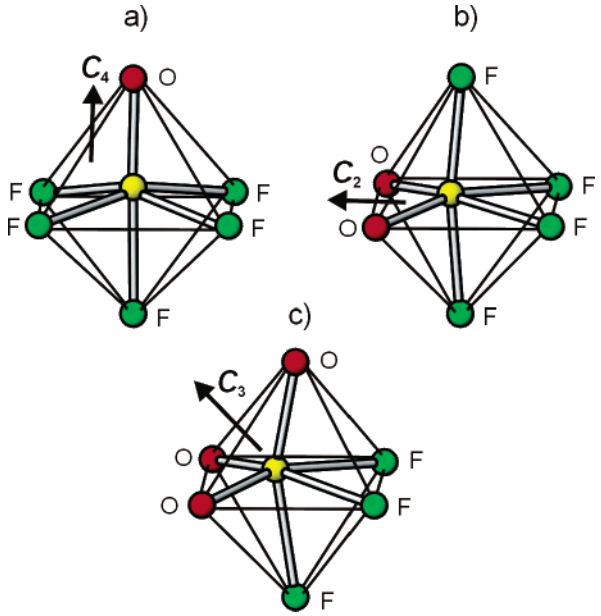

Figure 1. "Primary" out-of-center distortions of the octahedrally coordinated transition metal oxide fluoride anions which roughly coincide with (a) the C_4 rotational axis in $[MOF_5]^{2-}$, (b) the C_2 axis in $[MO_2F_4]^{2-}$, and (c) the C_3 axis in $[MoO_3F_3]^{3-}$.

* To whom correspondence should be addressed. E-mail: krp@northwestern.edu.

(1) Abrahams, S. C.; Reddy, J. M.; Bernstein, J. L. *J. Phys. Chem. Solids* **1966**, *27*, 997−1012.
(2) Zumsteg, F. C.; Bierlein, J. D.; Gier, T. E. *J. Appl. Phys.* **1976**, *47*, 4980−4985.
(3) Kunz, M.; Brown, I. D. *J. Solid State Chem.* **1995**, *115*, 395−406.
(4) Maggard, P. A.; Nault, T. S.; Stern, C. L.; Poeppelmeier, K. R. *J. Solid State Chem.* **2003**, *175*, 27−33.
(5) Griffith, W. P.; Wickins, T. D. *J. Chem. Soc. A* **1968**, 400−404.

10.1021/ic0502877 CCC: $30.25
Published on Web 05/28/2005

with the other oxide fluoride anions, there is a distinct displacement of the Mo^{6+} cation from the center of its octahedron toward the face shared by the three oxide ligands, resulting in a C_3 distorted anion. A similar local ordering has been observed in $Na_3MoO_3F_3$, in which oxides and fluorides are arranged in alternating planes: each Mo^{6+} is coordinated to three oxides and three fluorides and is shifted closer to the fac-oriented oxides.[6] This oxide and fluoride ordering has been suggested for the entire family of elpasolite-related $A_2BMO_3F_3$ (A, B = K^+, Rb^+, Cs^+; M = Mo^{6+}, W^{6+}) compounds.[7,8]

Although $[MO_xF_{6-x}]^{n-}$ anions that contain a single metal cation have been closely examined, far less is known about polyoxofluoroanions. Such compounds are similar in structure to the polyoxoanions commonly formed by molybdenum and tungsten.[9] In general, molybdenum(VI)- and tungsten(VI)-centered octahedra are found in corner- and edge-sharing environments within polyoxometalates but rarely crystallize in face-sharing structures.[10,11] However, several exceptions to this generalization have been identified experimentally: they include $Ba_3W_2O_9$[12] and $Ba_3Te_2O_9$,[13] which have similar confacial bioctahedral structures, and Cu(2,2′-bipyridine)$(Mo_2O_5)(O_3PCH_2CH_2CH_2PO_3)$, a layered organic−inorganic hybrid material that is constructed of face-sharing bioctahedral molybdates linked through copper-centered octahedra and phosphorus-centered tetrahedra.[14]

In this paper, the crystal structure of $[Cu(3\text{-apy})_4]_3(Mo_2O_6F_3)_2$ (3-apy = 3-aminopyridine) is reported and discussed. The discrete $[Mo_2O_6F_3]^{3-}$ anions contained in the crystal lattice are a rare example of face-sharing molybdenum(VI)-centered oxide fluoride polyhedra. Because of the crystallographic similarities between oxide and fluoride ions, one of the primary questions about the structure of the title compound concerns the specific locations of the oxide and fluoride ligands in either bridging or terminal sites of $[Mo_2O_6F_3]^{3-}$ confacial bioctahedra. This question will be addressed in several ways: first, the $[Mo_2O_6F_3]^{3-}$ bond lengths and angles will be characterized and compared to those found in a series of related oxide halide polyanions as well as the $[MoO_3F_3]^{3-}$ anion. The occupancies of the ligand sites will also be discussed in terms of the local electronic structure of an uncoordinated $[Mo_2O_6F_3]^{3-}$ anion and the results of molecular geometry optimization calculations.

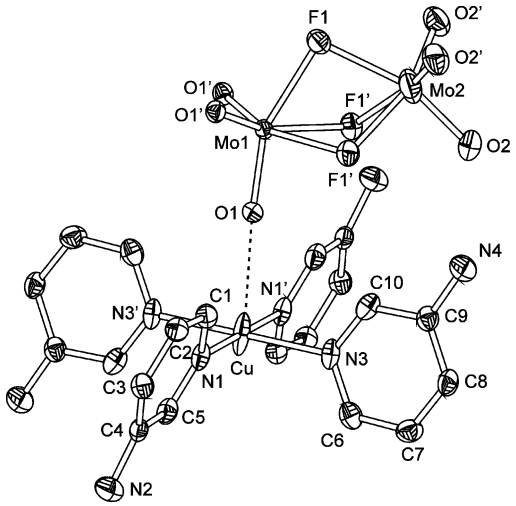

Figure 2. Thermal ellipsoid plot (showing 50% probability) of $[Cu(3\text{-apy})_4]_3(Mo_2O_6F_3)_2$.

Experimental Section

Caution! Hydrofluoric acid is both toxic and corrosive and must be handled with extreme caution and with the appropriate protective gear! If contact with the liquid or vapor occurs, proper treatment procedures should be followed immediately.[15−17]

Materials. CuO (99+%, Aldrich), MoO_3 (99.9995%, Alfa Aesar), 3-apy (99%, Aldrich), and aqueous hydrofluoric acid (HF) (49% HF by weight, Fisher) were used as received.

Synthesis. The highest yield of $[Cu(3\text{-apy})_4]_3(Mo_2O_6F_3)_2$ was obtained from the reaction of 0.0148 g (1.862×10^{-4} mol) of CuO, 0.0268 g (1.862×10^{-4} mol) of MoO_3, 0.3052 g (3.243×10^{-3} mol) of 3-apy, 0.0331 g (1.655×10^{-3} mol) of 49% HF, and 0.0992 g (5.505×10^{-3} mol) of deionized H_2O in a heat-sealed Teflon [fluoro(ethylene-propylene)] bag.[18] The bag was placed in a Teflon-lined 250-mL Parr autoclave, which was filled 33% with deionized H_2O as backfill, along with up to six other bags of varied composition. The autoclave was heated for 24 h at 150 °C and cooled to room temperature over an additional 24 h. The bag was opened in air, and the products were recovered by vacuum filtration. Green hexagonal crystals were recovered in ∼75% yield based on CuO.

Crystallographic Determination. Single-crystal X-ray diffraction data were collected with Mo Kα radiation (λ = 0.71073 Å) on a Bruker SMART-1000 CCD diffractometer and integrated with the SAINT-Plus program.[19] The structure was solved by direct methods and was refined via full-matrix least-squares techniques.[20] A face-indexed absorption correction was performed numerically via the program XPREP. The structure was checked for missing symmetry elements with PLATON.[21] The final refinement included anisotropic displacement parameters for the non-hydrogen atoms, which are shown in Figure 2. All hydrogen atoms, which were located on the 3-apy rings, were placed in calculated positions (C−H = 0.95 Å, N−H = 0.88 Å) and were refined via a riding

(6) Brink, F. J.; Norén, L.; Goossens, D. J.; Withers, R. L.; Liu, Y.; Xu, C.-N. *J. Solid State Chem.* **2003**, *174*, 450−458.
(7) Withers, R. L.; Welberry, T. R.; Brink, F. J.; Norén, L. *J. Solid State Chem.* **2003**, *170*, 211−220.
(8) Brink, F. J.; Norén, L.; Withers, R. L. *J. Solid State Chem.* **2003**, *174*, 44−51.
(9) Pope, M. T. *Heteropoly and Isopoly Oxometalates*; Springer-Verlag: New York, 1983.
(10) Bridgeman, A. J.; Cavigliasso, G. *J. Chem. Soc., Dalton Trans.* **2001**, 3556−3563.
(11) Cotton, F. A.; Wilkinson, G.; Murillo, C. A.; Bochmann, M. *Advanced Inorganic Chemistry*, 6th ed.; Wiley: New York, 1999; p 928.
(12) Poeppelmeier, K. R.; Jacobson, A. J.; Longo, J. M. *Mater. Res. Bull.* **1980**, *15*, 339−345.
(13) Jacobson, A. J.; Scanlon, J. C.; Poeppelmeier, K. R.; Longo, J. M.; Cox, D. E. *Mater. Res. Bull.* **1981**, *16*, 359−367.
(14) Finn, R. C.; Rarig, R. S., Jr.; Zubieta, J. *Inorg. Chem.* **2002**, *41*, 2109−2123.
(15) Bertolini, J. C. *J. Emerg. Med.* **1992**, *10*, 163−168.
(16) Peters, D.; Miethchen, R. *J. Fluorine Chem.* **1996**, *79*, 161−165.
(17) Segal, E. B. *Chem. Health Saf.* **2000**, *7*, 18−23.
(18) Harrison, W. T. A.; Nenoff, T. M.; Gier, T. E.; Stucky, G. D. *Inorg. Chem.* **1993**, *32*, 2437−2441.
(19) *SAINT-Plus*, version 6.02A; Bruker Analytical X-ray Instruments, Inc.: Madison, WI, 2000.
(20) Sheldrick, G. M. *SHELXTL*, version 5.10; Bruker Analytical X-ray Instruments, Inc.: Madison, WI, 1997.
(21) Spek, A. L. *PLATON*; Utrecht University: Utrecht, The Netherlands, 2001.

Table 1. Crystallographic Data

formula	$C_{60}H_{72}Cu_3F_6Mo_4N_{24}O_{12}$
fw	2009.80
space group	$R\bar{3}$ (No. 148)
a (Å)	13.881(1)
c (Å)	31.783(3)
V (Å^3)	5303.7(7)
Z	3
T (°C)	−120(1)
λ (Å)	0.71069
ρ_{calc} (g/cm^3)	1.888
ρ_{obsd}[a] (g/cm^3)	1.886(5)
μ (cm^{-1})	16.66
$R(F)$[b]	0.0401
$wR_2(F^2)$[c]	0.1014

[a] Density measurements by flotation pycnometry at 25 °C. [b] $R=\Sigma||F_o| - |F_c||/\Sigma|F_o|$. [c] $wR_2=[\Sigma w(F_o^2 - F_c^2)^2/\Sigma w(F_o^2)^2]^{1/2}$.

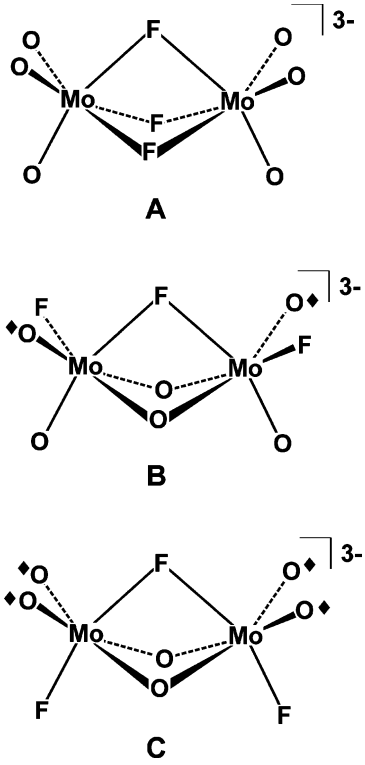

Figure 3. Three different ligand configurations for the $[Mo_2O_6F_3]^{3-}$ anion denoted as isomers A, B, and C. Terminal oxide ligands that are trans to bridging metal−oxide bonds are denoted by a filled diamond (◆).

model with isotropic displacement parameters constrained to equal 1.2 times the equivalent isotropic displacement parameter of the parent atom. See Table 1 for crystallographic data and the Supporting Information for the crystallographic information file.

Spectroscopic Measurements. A mid-infrared (400−4000 cm^{-1}) spectrum on a $[Cu(3\text{-apy})_4]_3(Mo_2O_6F_3)_2$ sample that had been ground and pelletized with dried KBr was obtained via a Bio-Rad FTS-60 FTIR spectrometer operating at a 2-cm^{-1} resolution.

Computational Study. Geometry optimizations were performed on the three uncoordinated $[Mo_2O_6F_3]^{3-}$ anions with the different ligand arrangements shown in Figure 3. The geometries of these $[Mo_2O_6F_3]^{3-}$ isomers were optimized via implementation of the restricted Hartree−Fock (RHF) method in GAMESS-US[22] using built-in 3-21G basis sets. Subsequent electronic structure calculations of uncoordinated $[Mo_2O_6F_3]^{3-}$ molecular anions, which were based on the crystallographically determined coordinates for a $[Mo_2O_6F_3]^{3-}$ unit within $[Cu(3\text{-apy})_4]_3(Mo_2O_6F_3)_2$ and on the RHF-optimized coordinates for uncoordinated $[Mo_2O_6F_3]^{3-}$ anions, were carried out via the Fenske−Hall (FH) molecular orbital method.[23] The results of the FH calculations on $[Mo_2O_6F_3]^{3-}$ anions were used to determine atomic charges and the relative σ and π components of Mo=O and Mo−F bond overlap populations via Mulliken population analyses.[24,25]

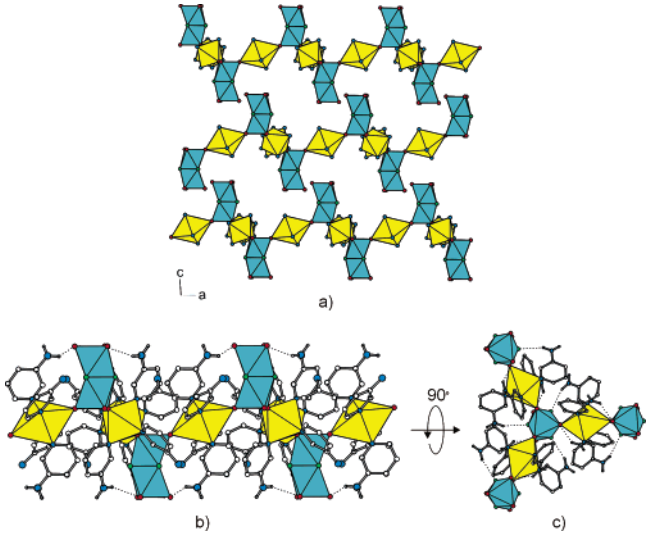

Figure 4. Packing diagram of $[Cu(3\text{-apy})_4]_3(Mo_2O_6F_3)_2$ showing (a) the separate layers of anions and cations, (b) a single layer, and (c) coordination around the anion. Yellow polyhedra represent octahedrally coordinated Cu^{2+}, and blue polyhedra represent octahedrally coordinated Mo^{6+}.

Atomic basis functions for FH calculations were obtained by a best fit to Herman−Skillman atomic calculations[26] using the method of Bursten, Jensen, and Fenske.[27] The 5s and 5p functions were given exponents of 2.2 for Mo. Valence 2p functions for O and F were retained as double-ζ functions. See Supporting Information for atomic coordinates and output files.

Results

The three-dimensional extended structure of $[Cu(3\text{-apy})_4]_3(Mo_2O_6F_3)_2$, shown in Figure 4a, is built up from $[Cu(3\text{-apy})_4]^{2+}$ cations and $[Mo_2O_6F_3]^{3-}$ anions. The $[Mo_2O_6F_3]^{3-}$ anion is made up of two face-sharing octahedra with a Mo−Mo distance of 3.171(1) Å. The long bridging positions are assigned as fluorides, which results in long bonds of Mo1−F1 (2.181(2) Å × 3) and Mo2−F1 (2.113(2) Å × 3). The terminal positions are assigned as oxides to provide bond lengths of Mo1=O1 = 1.747(2) Å × 3 and Mo2=O2 = 1.770(3) Å × 3. The Jahn−Teller distorted Cu^{2+} is coordinated to four 3-apy rings in the equatorial positions with Cu−N1 = 2.034(3) Å × 2 and Cu−N3 = 2.043(3) Å × 2, whereas the axial positions are occupied by oxide ligands from $[Mo_2O_6F_3]^{3-}$ units at a Cu−O1 distance of 2.624(2) Å × 2. Selected bond distances and angles are listed in Table 2.

(22) Schmidt, M. W.; Baldridge, K. K.; Boatz, J. A.; Elbert, S. T.; Gordon, M. S.; Jensen, J. H.; Koseki, S.; Matsunaga, N.; Nguyen, K. A.; Su, S. J.; Windus, T. L.; Dupuis, M.; Montgomery, J. A. *J. Comput. Chem.* **1993**, *14*, 1347−1363.

(23) Hall, M. B.; Fenske, R. F. *Inorg. Chem.* **1972**, *11*, 768−775.
(24) Mulliken, R. S. *J. Chem. Phys.* **1955**, *23*, 1833−1840.
(25) Mulliken, R. S. *J. Chem. Phys.* **1955**, *23*, 1841−1846.
(26) Herman, F.; Skillman, S. *Atomic Structure Calculations*; Prentice Hall: Englewood Cliffs, NJ, 1963.
(27) Bursten, B. E.; Jensen, J. R.; Fenske, R. F. *J. Chem. Phys.* **1978**, *68*, 3320−3321.

Table 2. Bond Valence Sums,[a] Calculated Mulliken Charges, and Selected Bond Angles

bond	length (R_i, Å)	valence (S_i)[b]	residual charge[c]	Mulliken charge[d]	bond angle	degrees
			$[Cu(3\text{-apy})_4]_3(Mo_2O_6F_3)_2$			
Mo1═O1 × 3	1.747(2)	1.54	−0.46	−0.83	Mo1−F1−Mo2	95.2(1)
Mo1−F1 × 3	2.181(2)	0.37	−0.19	−0.52	O1−Mo1−O1′	103.8(1)
ΣS_{Mo}		5.73			O2−Mo2−O2′	101.1(1)
Mo2═O2 × 3	1.770(3)	1.45	−0.55	−0.85	F1−Mo1−F1′	70.18(8)
Mo2−F1 × 3	2.113(2)	0.44	−0.19	−0.52	F1−Mo2−F1′	72.78(8)
ΣS_{Mo}		5.67				
			$(Ag_3MoO_3F_3)(Ag_3MoO_4)Cl$			
Mo═O × 3	1.755(6)	1.51	−0.49	−0.95	O−Mo−O	103.1(3)
Mo−F × 3	2.083(5)	0.48	−0.52	−0.69	F−Mo−F	77.3(2)
ΣS_{Mo}		5.97				

[a] Bond valence calculated with the program *Bond Valence Calculator*, version 2.00; Hormillosa, C., Healy, S., Stephen, T.; McMaster University, 1993. [b] Valence sums calculated with the formula: $S_i = \exp[(R_0 - R_i)/B]$, in which S_i = the valence of bond i, R_0 = the constant dependent on the bonded elements, R_i = the bond length of bond i, and $B = 0.370$. ΣS_{Mo} = the bond valence sum for the metal. $R_0(Mo{-}O) = 1.907$ and $R_0(Mo{-}F) = 1.808$. [c] Ligand residual charge = $V_i - S_i$, in which V_i = the oxidation state for ligand i. The residual charge on F1 was calculated as described in the text. [d] As determined by FH calculations. Extrapolation limit = 0.001.

The structure of $[Cu(3\text{-apy})_4]_3(Mo_2O_6F_3)_2$ is composed of neutral layers. $[Cu(3\text{-apy})_4]^{2+}$ cations make up the positive core of each layer, while the negative top and bottom of the layer consist of regularly placed $[Mo_2O_6F_3]^{3-}$ anions (see Figure 4b). There are two $[Mo_2O_6F_3]^{3-}$ anions for every three $[Cu(3\text{-apy})_4]^{2+}$ cations within a single layer; thus, the overall charge is balanced, and the stoichiometry of the compound is maintained. The amino substituents on the 3-apy rings provide hydrogen-bonding donors: these amino groups are oriented toward the negative top and bottom of each layer such that extensive intralayer hydrogen bonding with both the bridging and the terminal ligands on the face-sharing bioctahedra can occur. A hydrogen bond is made from an amino group to each terminal O2 from the three $[Cu(3\text{-apy})_4]^{2+}$ cations coordinated to each $[Mo_2O_6F_3]^{3-}$ anion at $d(N4{-}H\cdots O2) = 2.958$ Å. Each F1 ligand can form two hydrogen bonds to two different $[Cu(3\text{-apy})_4]^{2+}$ cations at $d(N2{-}H\cdots F1) = 3.221$ Å and $d(N4{-}H\cdots F1) = 3.374$ Å. Additionally, interlayer hydrogen bonding connects the layers together at $d(N2{-}H\cdots O2) = 3.315$ Å (see Figure 4c).

The infrared spectrum of $[Cu(3\text{-apy})_4]_3(Mo_2O_6F_3)_2$ shows two peaks of equal intensity at 887 and 860 cm^{-1}, which are assigned to stretches of the hydrogen- and copper-bonded Mo═O, respectively. A peak at 828 cm^{-1} is attributed to the asymmetrical stretching of the O−Cu−O group,[28] and a Mo−F−Mo peak appears at 727 cm^{-1}. Additional peaks at 3450, 3330, 1619, 1492, 1442, 1319, 797, 698, and 654 cm^{-1} are indicative of 3-apy coordinated to copper.[29]

Discussion

The $[Mo_2O_6F_3]^{3-}$ anion has been reported previously in the crystal structure of $Cs_3Mo_2O_6F_3$.[30] Nearly identical to the molecular anion in $[Cu(3\text{-apy})_4]_3(Mo_2O_6F_3)_2$, as indicated by the bond lengths and angles listed in Table 3, the crystal structure refinement of $[Mo_2O_6F_3]^{3-}$ in $Cs_3Mo_2O_6F_3$ places the terminal and bridging positions of the bioctahedral unit

Table 3. Comparison of Bond Lengths (Å) and Angles (°) in $Cs_3Mo_2O_6F_3$[a] and $[Cu(3\text{-apy})_4]_3(Mo_2O_6F_3)_2$[b]

		$[Cu(3\text{-apy})_4]_3(Mo_2O_6F_3)_2$	
	$Cs_3Mo_2O_6F_3$	(Mo1)	(Mo2)
Mo−X_t	1.76	1.75	1.79
Mo−X_b	2.15	2.18	2.11
Mo−Mo	3.20	3.17	
X_t−Mo−X_t	103.9	103.7	100.7
X_b−Mo−X_b	70.6	70.1	72.7
Mo−X_b−Mo	96.2	95.3	

[a] Ref 30. [b] The subscripts "t" and "b" refer to terminal and bridging ligands, respectively.

at distances of 1.757(8) Å × 6 and 2.152(4) Å × 3, respectively, from the molybdenum centers. Mattes et al. concluded that the six oxide and three fluoride ligands in $Cs_3Mo_2O_6F_3$ were statistically disordered over the nine positions and stated incorrectly that this completely disordered model would simultaneously minimize electrostatic repulsions between the molybdenum cations while allowing for a favorable cis arrangement of the dioxo groups around molybdenum.

A comparison of the bond lengths and angles given in Table 3 indicates that the disordered $[Mo_2O_6F_3]^{3-}$ model and our ordered model in $[Cu(3\text{-apy})_4]_3(Mo_2O_6F_3)_2$ share a number of structural similarities. However, if ligand disorder were to occur in $[Cu(3\text{-apy})_4]_3(Mo_2O_6F_3)_2$, the thermal ellipsoids would be elongated along the Mo−ligand bonds. As shown in Figure 2, this is not the case: both terminal and bridging ligand positions feature nearly spherical ellipsoids. Comparisons of $[Mo_2O_6F_3]^{3-}$ with other oxide halide systems and the results of electronic structure calculations, which are discussed in greater detail below, also lead us to conclude that an ordered model for the $[Mo_2O_6F_3]^{3-}$ anion in $[Cu(3\text{-apy})_4]_3(Mo_2O_6F_3)_2$ is more probable. Furthermore, these studies indicate that the six oxide ligands should be assigned to terminal positions and the three fluorides should be assigned to bridging positions within the anion.

Related Oxide Halide Polyanionic Structures. A comparison of the $[Cu(3\text{-apy})_4]_3(Mo_2O_6F_3)_2$ crystal structure with other oxyhalide structures that have similar, yet well-characterized, ligand geometries can provide useful informa-

(28) Chertihin, G. V.; Andrews, L.; Bauschlicher, C. W., Jr. *J. Phys. Chem. A* **1997**, *101*, 4026−4034.
(29) Akyuz, S. *J. Mol. Struct.* **1998**, *449*, 23−27.
(30) Mattes, R.; Mennemann, K.; Jaeckel, N.; Rieskamp, H.; Brockmeyer, H. J. *J. Less-Common Met.* **1980**, *76*, 199−212.

tion and insight about the structure of the $[Mo_2O_6F_3]^{3-}$ anion. One such example is the $[Mo_4O_{12}F_3]^{3-}$ oxide fluoride polyanion in $(Me_4N)_3(Mo_4O_{12}F_3)\cdot 0.8H_2O$, which features both terminal and bridging oxide ligands.[31] The Mo═O bonds in $[Mo_4O_{12}F_3]^{3-}$ are ~1.7 Å in length. The bridging oxide positions are further from the metal centers at a distance of 1.9 Å, while the bridging metal−fluoride bond length is 2.2 Å. Another compound, $[(n\text{-}C_4H_9)_4N]_2(Mo_2O_5Cl_4)\cdot(C_2H_5)_2O$, contains face-sharing bioctahedral $[Mo_2O_5Cl_4]^{2-}$ anions.[32] Because of differences in size and electron density, the oxide and chloride ligands can be differentiated from one another with a higher degree of certainty than can oxide and fluoride ligands. The crystal structure of $[(n\text{-}C_4H_9)_4N]_2(Mo_2O_5Cl_4)\cdot 1/3(C_2H_5)_2O$ reveals that the four chloride ligands in $[Mo_2O_5Cl_4]^{2-}$ are all positioned trans to an oxide. This results in confacial bioctahedra that contain both bridging and terminal oxide ligands. Each of the four terminal oxides in $[Mo_2O_5Cl_4]^{2-}$ is approximately 1.7 Å from its respective metal cation, whereas the single bridging oxide is ~1.9 Å from the Mo^{6+} centers.

In all, both $(Me_4N)_3(Mo_4O_{12}F_3)\cdot 0.8H_2O$ and $[(n\text{-}C_4H_9)_4N]_2(Mo_2O_5Cl_4)\cdot 1/3(C_2H_5)_2O$ have terminal Mo═O bonds that are 1.7 Å in length; this value corresponds well to the $[Mo_2O_6F_3]^{3-}$ terminal metal−ligand bond lengths of 1.747 and 1.770 Å. However, at 2.113 and 2.181 Å the bridging metal−ligand bonds in $[Mo_2O_6F_3]^{3-}$ are considerably longer than the 1.9-Å bridging Mo−O bonds in the two example structures. These important structural comparisons support the assignment of the oxide ligands to the terminal positions of the $[Mo_2O_6F_3]^{3-}$ anion in both $[Cu(3\text{-apy})_4]_3(Mo_2O_6F_3)_2$ and $Cs_3Mo_2O_6F_3$.

Comparison of $[Mo_2O_6F_3]^{3-}$ with $[MoO_3F_3]^{3-}$. As noted earlier, the $[MoO_3F_3]^{3-}$ anions in $(Ag_3MoO_3F_3)(Ag_3MoO_4)$-Cl undergo an inherent "primary" distortion as each Mo^{6+} moves out of the center of its octahedron toward the three fac oxide ligands[4] (bond lengths and angles are listed in Table 2). One of the significant structural features of the $[MoO_3F_3]^{3-}$ anion is that the O−Mo−O angles between the terminal oxide ligands are all greater than 90°, as shown in Table 2. A similar bond angle expansion is observed in the closely related $[MoO_2F_4]^{2-}$ anion, in which the angle between the two cis oxide ligands is ~102°.[33−35] Such an expansion is related to a number of factors, including the trans effects of oxide ligands, which allow for strong oxide−metal bonds at the expense of the bond trans to the oxide. The double bond character of the metal−oxide bonds draws the oxides closer to the central metal atom and increases steric repulsions between the ligands. As a result, the O−Mo−O angles in the $[MoO_3F_3]^{3-}$ anion are expanded to the extent that their magnitude more closely resembles the angles in compounds with *tetrahedrally* coordinated metal cations, rather than those observed in regular octahedral coordination.

Table 4. Calculated Bond Overlap Populations[a] for $[MoO_3F_3]^{3-}$ and $[Mo_2O_6F_3]^{3-}$ [b]

	$[MoO_3F_3]^{3-}$	$[Mo_2O_6F_3]^{3-}$
Mo−O σ	0.413	0.438
Mo−O π	0.408	0.455
Mo−O total ($\sigma + \pi$)	0.821	0.893
% Mo−O 2s character	16.6	17.4
Mo−F σ	0.236	0.195
Mo−F π	0.044	0.012
Mo−F total ($\sigma + \pi$)	0.280	0.207
% Mo−F 2s character	5.82	3.70

[a] As determined by FH calculations. Extrapolation limit = 0.001. [b] Reported populations show the σ and π contributions to the metal−ligand bonds as well as the ligand 2s orbital contribution to both. Values reported for $[Mo_2O_6F_3]^{3-}$ represent the average value of interactions with the two unique Mo^{6+} sites.

According to Pauling's second crystal rule, ligands with more negative oxidation states will occupy sites with larger bond valence sums.[36] Bond valence calculations[37,38] for the $[MoO_3F_3]^{3-}$ anion, as listed in Table 2, reveal that the short bonds between the Mo^{6+} centers and the oxide ligands have multiple bond character. This is indicated by the Mo═O bond valences that are greater than 1. Bond overlap populations, which reflect the amount of electron density shared between two bonded atoms, serve as another useful tool for quantitative comparisons of covalent bond strength. Listed for both $[MoO_3F_3]^{3-}$ and $[Mo_2O_6F_3]^{3-}$ in Table 4, bond overlap populations indicate that the strong, short Mo═O bonds have significant π character, whereas the longer Mo−F bonds trans to the oxides are, as expected, less covalent.

Within the $[Cu(3\text{-apy})_4]_3(Mo_2O_6F_3)_2$ crystal structure, the terminal ligand positions of the $[Mo_2O_6F_3]^{3-}$ anions are significantly closer to the Mo^{6+} centers than are the bridging positions, as indicated by a comparison of the Mo═O and Mo−F bond lengths. Additionally, the bond angles between the terminal positions are significantly larger than 90°, whereas the bond angles between the bridging ligands are closer to 70° (see Table 2). Overall, the short terminal metal−ligand bonds, long metal−ligand−metal bridging interactions, and bond angles within a $[Mo_2O_6F_3]^{3-}$ anion result in a configuration with two Mo^{6+} cations in bonding environments that are remarkably similar to those found in two $[MoO_3F_3]^{3-}$ anions that have been aligned such that their three fac fluoride ligands are bridging. This structure would place oxide ligands exclusively on terminal sites and is concurrent with the other oxide fluoride anions in which the primary distortion occurs toward the oxide ligands.

Bond valence calculations for the $[Mo_2O_6F_3]^{3-}$ anion, listed in Table 2, also support this ligand arrangement. The presence of bridging ligands within $[Mo_2O_6F_3]^{3-}$ must be considered when bond valences and residual negative charges

(31) Buchholz, N.; Mattes, R. *Angew. Chem., Int. Ed. Engl.* **1986**, *25*, 1104−1105.
(32) Ozeki, T.; Sakaguchi, M.; Yagasaki, A. *Polyhedron* **2000**, *18*, 43−45.
(33) Heier, K. R.; Norquist, A. J.; Wilson, C. G.; Stern, C. L.; Poeppelmeier, K. R. *Inorg. Chem.* **1998**, *37*, 76−80.
(34) Maggard, P. A.; Stern, C. L.; Poeppelmeier, K. R. *J. Am. Chem. Soc.* **2001**, *123*, 7742−7743.
(35) Maggard, P. A.; Kopf, A. L.; Stern, C. L.; Poeppelmeier, K. R.; Ok, K. M.; Halasyamani, P. S. *Inorg. Chem.* **2002**, *41*, 4852−4858.
(36) Tobias, G.; Beltran-Porter, D.; Lebedev, O. I.; Van Tendeloo, G.; Rodriguez-Carvajal, J.; Fuertes, A. *Inorg. Chem.* **2004**, *43*, 8010−8017.
(37) Brown, I. D.; Altermatt, D. *Acta Crystallogr., Sect. B* **1985**, *41*, 244−247.
(38) Brese, N. E.; O'Keeffe, M. *Acta Crystallogr., Sect. B* **1991**, *47*, 192−197.

are evaluated, as bond valence calculations are specifically designed for classic, two-center bonds. Because each fluoride forms bonds to *both* of the molybdenum centers in $[Mo_2O_6F_3]^{3-}$, the net residual negative charge localized on a fluoride ligand will be equivalent to the oxidation state of fluoride (1) subtracted by the Mo−F bond valences from both ($MoO_3F_{3/2}$) units. When the fluoride charges are evaluated in this manner, they are found to be much lower than the charge on the oxide ligands. This observation, which is also supported by the Mulliken charges listed in Table 2, is consistent with other transition metal oxide fluoride compounds that consist of $[MO_xF_{6-x}]^{n-}$ anions and $[ML_4]^{2+}$ cations in which the anion is linked to the cation through the ligand(s) with the greatest negative charge.[33,39−41] When oxides are assigned to terminal positions in $[Mo_2O_6F_3]^{3-}$, this preferential coordination is observed in $[Cu(3\text{-apy})_4]_3(Mo_2O_6F_3)_2$, in which each of the O1 oxides coordinates to a $[Cu(3\text{-apy})_4]^{2+}$. The O2 ligands, which have slightly less negative charges, participate in hydrogen bonding. With still less negative charges, the fluoride ligands also participate in hydrogen bonding but at longer distances than do the oxides: the average distance of the intralayer fluoride hydrogen bond interactions is $d(N-H\cdots F1) = 3.30$ Å, whereas the intralayer O2 hydrogen bonds occur at a distance of 2.958 Å.

Metal−Metal Separation in Face-Sharing Bioctahedral (FSBO) Structures. There have been numerous analyses of metal−metal bonding within FSBO structures which relate the strength of the metal−metal interactions to the overall geometry of the bioctahedra.[42] A classic, often-cited example of this relationship is illustrated by the comparison of the confacial bioctahedral $[Cr_2Cl_9]^{3-}$ and $[W_2Cl_9]^{3-}$ anions. It has been shown that although $[Cr_2Cl_9]^{3-}$ and $[W_2Cl_9]^{3-}$ are isoelectronic to one another, $[W_2Cl_9]^{3-}$ contains a metal−metal bond, whereas $[Cr_2Cl_9]^{3-}$ does not.[43−47] This electronic structure difference is physically manifested by the relative out-of-center distortions exhibited by the metal atoms; that is, the overall "length" of a $[Cr_2Cl_9]^{3-}$ anion is almost identical to that of two Cr-centered octahedra, whereas the W−W interaction in $[W_2Cl_9]^{3-}$ shortens the FSBO anion considerably.

Unlike these $[M_2Cl_9]^{3-}$ examples, there are no electrons available for metal−metal bonding in the $[Mo_2O_6F_3]^{3-}$ anions, and as expected, the calculated bond overlap population for the Mo−Mo interaction in an uncoordinated $[Mo_2O_6F_3]^{3-}$ anion is effectively zero. The presence of two highly charged Mo^{6+} centers within a single anion introduces a strong, energetically unfavorable cation−cation repulsion. Thus, it is not surprising that the general shape of the FSBO $[Mo_2O_6F_3]^{3-}$ anion, with a long metal−metal distance and a Mo1−ligand−Mo2 angle close to 90°, more closely resembles the $[Cr_2Cl_9]^{3-}$ anion than it does $[W_2Cl_9]^{3-}$: in this geometry, Mo−Mo repulsions are minimized. One of the consequences of a large metal−metal separation, however, is that the resulting FSBO anion exhibits bridging metal−ligand bonds that are also quite long. On the basis of the previous comparisons of both terminal and bridging M−O bond lengths in $(Me_4N)_3(Mo_4O_{12}F_3)\cdot 0.8H_2O$ and $[(n\text{-}C_4H_9)_4N]_2(Mo_2O_5Cl_4)\cdot 1/3(C_2H_5)_2O$, it is unlikely that oxides would preferentially occupy the bridging positions in $[Mo_2O_6F_3]^{3-}$, as this would result in Mo−O bonds over 2.0 Å in length. Furthermore, when oxides are assigned to the terminal sites in $[Mo_2O_6F_3]^{3-}$, the primary distortions in each of the individual ($MoO_3F_{3/2}$) units are preserved. In this configuration, both Mo^{6+} cations are displaced away from one another and move closer to their respective three fac oxide ligands.

Covalency of Terminal vs Bridging Ligand Sites in FSBO Structures. The likelihood that oxide and fluoride ligands respectively occupy terminal and bridging sites in $[Mo_2O_6F_3]^{3-}$ can be further examined by considering the general orbital structure of confacial bioctahedra. In 1979, Summerville and Hoffmann carried out thorough electronic structure analyses of M_2L_9 complexes, taking into account the effects of ligand electron donating or withdrawing ability on the shape and relative energy levels of the frontier orbitals within an FSBO structure.[48] Many parallels can be drawn between these earlier studies of FSBO anions with electron donor ligands and the structure of the $[Mo_2O_6F_3]^{3-}$ anion.

Figure 5 provides a generalized picture of two of the molecular orbitals that contribute to the bridging metal−ligand−metal interactions in a $M_2(CO)_6(\mu\text{-}X)_3$ complex, where X is a π-donating ligand.[48] The molecular orbitals drawn in Figure 5 represent those for an FSBO anion with six π-accepting CO ligands in terminal positions; however, they are almost identical in shape to their counterparts in $[Mo_2O_6F_3]^{3-}$, which has π-donor ligands in the terminal positions. Only the interactions between ligand 2p and the metal valence orbitals are shown in Figure 5, as the low energies of oxygen and, in particular, fluorine 2s orbitals inhibit significant ligand 2s contribution to the overall metal−ligand bonding. Upon examination of these molecular orbitals, it becomes apparent that the metal-bridging ligand overlap will decrease as the metal−metal distance increases. In particular, as the separation between the metal atoms increases the ligand orbitals in the a_2'' molecular orbital will move into the radial nodes of the primarily d_{z^2}-based metal orbitals.

This relationship between metal−metal separation and bridging metal−ligand−metal overlap strongly suggests that

(39) Halasyamani, P.; Willis, M. J.; Stern, C. L.; Lundquist, P. M.; Wong, G. K.; Poeppelmeier, K. R. *Inorg. Chem.* **1996**, *35*, 1367−1371.
(40) Halasyamani, P. S.; Heier, K. R.; Norquist, A. J.; Stern, C. L.; Poeppelmeier, K. R. *Inorg. Chem.* **1998**, *37*, 369−371.
(41) Welk, M. E.; Norquist, A. J.; Stern, C. L.; Poeppelmeier, K. R. *Inorg. Chem.* **2000**, *39*, 3946−3947.
(42) Cotton, F. A.; Ucko, D. A. *Inorg. Chim. Acta* **1972**, *6*, 161−172 and references therein.
(43) Cotton, F. A. *Rev. Pure Appl. Chem.* **1967**, *17*, 25−40.
(44) Kraatz, H.-B.; Boorman, P. M. *Coord. Chem. Rev.* **1995**, *143*, 35−69.
(45) Lovell, T.; McGrady, J. E.; Stranger, R.; Macgregor, S. A. *Inorg. Chem.* **1996**, *35*, 3079−3080.
(46) McGrady, J. E.; Lovell, T.; Stranger, R. *Inorg. Chem.* **1997**, *36*, 3242−3247.
(47) McGrady, J. E.; Stranger, R.; Lovell, T. *J. Phys. Chem. A* **1997**, *101*, 6265−6272.
(48) Summerville, R. H.; Hoffmann, R. *J. Am. Chem. Soc.* **1979**, *101*, 3821−3831.

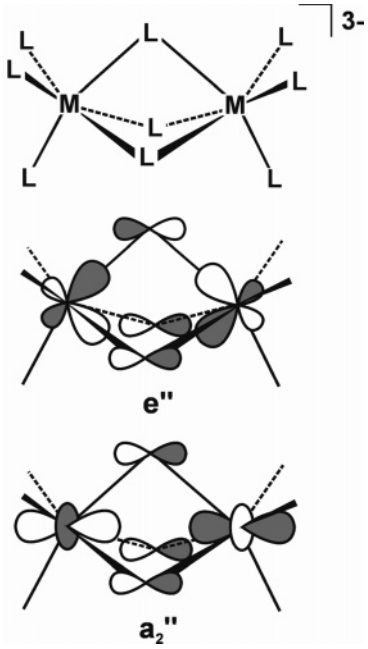

Figure 5. Generalized schematic of two of the molecular orbitals primarily responsible for the bridging metal−ligand−metal interactions in an FSBO anion (adapted from ref 48).

the relative covalency of the bridging sites decreases as the overall length of an FSBO anion increases. At the same time, the relative distance between the metal atoms has very little effect on the strength of the metal−terminal ligand bonds. The rather long Mo−Mo distance of 3.17 Å in $[Mo_2O_6F_3]^{3-}$ implies that the metal-bridging ligand overlap is rather weak and that the bridging sites are therefore better suited for the more electronegative fluoride ligands: this would leave the oxide ligands to form more covalent terminal bonds with the Mo^{6+} centers. Calculated bond overlap populations (Table 4) not only confirm that the Mo═O bonds in $[Mo_2O_6F_3]^{3-}$ are considerably more covalent than are the Mo−F bonds, but that there is significant π contribution to the terminal metal−ligand bonding, as well. Thus, a fluoride that occupies one of the two-coordinate bridging positions in $[Mo_2O_6F_3]^{3-}$ is still in a *less* covalent bonding environment than that of a singly coordinated terminal ligand.

Geometry Optimizations of $[Mo_2O_6F_3]^{3-}$. Hartree−Fock geometry optimizations have been carried out on uncoordinated $[Mo_2O_6F_3]^{3-}$ anions with the three different ligand configurations shown in Figure 3. These model isomers were constructed by taking coordinates for the FSBO anion directly from the $[Cu(3\text{-apy})_4]_3(Mo_2O_6F_3)_2$ crystallographic data and designating each ligand as either a fluoride or an oxide. Isomer "A" is a $[Mo_2O_6F_3]^{3-}$ model in what we believe is the most probable configuration, with fluorides exclusively in bridging positions and six terminal oxide ligands. The ligand distributions in isomers "B" and "C" more closely reflect the model suggested by Mattes et al. for a statistically disordered $[Mo_2O_6F_3]^{3-}$ anion in $Cs_3Mo_2O_6F_3$, in which each ligand site has an average composition of $2/3O^{2-}/1/3F^-$. Both B and C have one bridging and two terminal fluoride ligands. In isomer B, the fluorides are distributed such that none of them are trans to another, whereas in C all three fluorides are trans to each other.

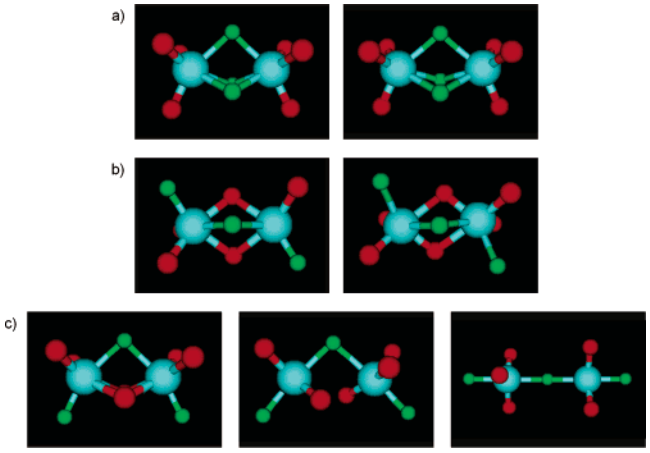

Figure 6. Input (left) and output (right) geometries that depict the RHF minimum energy atomic configurations of different $[Mo_2O_6F_3]^{3-}$ isomers. The structures shown in (a), (b), and (c) respectively correspond to isomers A, B, and C, as illustrated in Figure 3. Models were generated with the program MOLDEN.[49] The oxide and fluoride coloring scheme is the same as that used in Figure 1.

Table 5. A Comparison of Bond Lengths (Å) for the Crystallographically Determined $[Mo_2O_6F_3]^{3-}$ Anion in $[Cu(3\text{-apy})_4]_3(Mo_2O_6F_3)^{3-}$ and RHF Geometry Optimized $[Mo_2O_6F_3]^{3-}$ Anions with Different Ligand Configurations

	$[Mo_2O_6F_3]^{3-}$ from experiment	isomer A FSBO, 3 bridging F^-	isomer B FSBO, 2 terminal, 1 bridging F^-	isomer C corner-sharing bipyramids
$Mo-O_t$	1.759	1.733	1.727	1.737
$Mo-O_b$			1.811	
			2.241	
$Mo-F_t$			1.968	1.988
$Mo-F_b$	2.147	2.173	2.228	2.107
Mo−Mo	3.171	3.351	3.059	

Figure 6 summarizes the results of geometry optimizations on the three uncoordinated $[Mo_2O_6F_3]^{3-}$ isomers.[49] The calculated minimum energy structure of isomer A, depicted in Figure 6a, is very similar to the crystallographically determined geometry of the molecular anion in $[Cu(3\text{-apy})_4]_3(Mo_2O_6F_3)_2$. A comparison of the bond lengths and angles in the experimental and theoretical models (Table 5) indicates that geometry optimizations make only slight changes to the structure of $[Mo_2O_6F_3]^{3-}$: the theoretical isomer A has slightly shorter terminal Mo═O bonds and longer Mo−F bonds, but the overall connectivity of the atoms remains the same as that of the FSBO anion in its crystal structure. In contrast, the results of calculations on isomers B and C demonstrate an important consequence of placing fluoride ligands in terminal positions within $[Mo_2O_6F_3]^{3-}$: both of these configurations force oxide ligands into sites that are trans to other oxides. The input structure for isomer B has two terminal oxide ligands that are trans to bridging oxides, as designated by the filled diamonds (◆) in Figure 3b. Over the course of the calculation, each of the two bridging oxide ligands moves away from its respective trans oxide toward opposing Mo^{6+} centers. This movement is also reflected in

(49) Schaftenaar, G.; Noordik, J. H. MOLDEN, A Pre- and Postprocessing Program for Molecular and Electronic Structures. In *J. Comput.-Aided Mol. Des.* **2000**, *14*, 123−134.

the bond lengths listed in Table 5. The destabilizing trans effects of oxide ligands are so pronounced in isomer C, in which all six of the oxides are trans to one another, that the bridging Mo−O−Mo interactions are broken (see Figure 6c). The lone remaining Mo−F−Mo bridging interaction subsequently straightens to approximately 180°, resulting in a final minimum energy structure that is best described as a pair of trigonal bipyramids joined by the single bridging fluoride ligand. In both bipyramids, oxide ligands occupy equatorial positions, and fluorides occupy axial sites.

These results suggest that a bridging Mo−O−Mo interaction is less stable than a Mo−F−Mo interaction in $[Mo_2O_6F_3]^{3-}$. In addition to the oxide ligand trans effect, this instability is related to a general periodic trend: from left to right across the periodic table, the relative energy level separation of the s and p valence orbitals increases. As a result, oxygen atoms participate in more sp mixing than do fluorine atoms. It has been noted that the tendency of electron-rich three-center systems to localize into a bond and a lone pair is closely related to the extent of the sp mixing that occurs in the central, or bridging, atom.[50] The relative contributions of ligand 2s orbitals to metal−ligand bonds in $[Mo_2O_6F_3]^{3-}$, as determined by bond overlap populations, are given in Table 4. These percentages show that the Mo═O bonds have a significantly greater degree of 2s character than do the Mo−F interactions. This suggests that the actual "shapes" of the oxide orbitals used to bond to the Mo^{6+} centers more closely resemble those of sp hybrids than those of pure 2p orbitals. Thus, if oxide ligands were to occupy bridging sites within $[Mo_2O_6F_3]^{3-}$, electrons localized on the bridging oxides would occupy orbitals that are directed at either one metal center or another.

It is important to note that the specific ligand ordering in isomer A is the only possible configuration of the $[Mo_2O_6F_3]^{3-}$ anion that eliminates all trans O−Mo−O interactions. The aforementioned FSBO anion $[Mo_2O_5Cl_4]^{2-}$, isolated in $[(n\text{-}C_4H_9)_4N]_2(Mo_2O_5Cl_4)\cdot 1/3(C_2H_5)_2O$, contains both bridging and terminal chloride ligands; however, the specific stoichiometry of $[Mo_2O_5Cl_4]^{2-}$ is such that the halide ligands can occupy both bridging and terminal sites without resulting in any trans O−Mo−O interactions. The results of these Hartree−Fock calculations therefore suggest that the most energetically feasible model for an FSBO structure with the same stoichiometry as $[Mo_2O_6F_3]^{3-}$ will be one in which all three fluorides occupy bridging sites and all six oxides are in terminal positions.

(50) Munzarová, M. L.; Hoffmann, R. *J. Am. Chem. Soc.* **2002**, *124*, 4787−4795.

Conclusions

Experimental and computational techniques have been used to characterize the FSBO anion $[Mo_2O_6F_3]^{3-}$ in the new compound $[Cu(3\text{-apy})_4]_3(Mo_2O_6F_3)_2$. These studies all suggest that the six terminal positions of the anion are occupied by oxide ligands and the three fluoride ligands occupy the bridging positions between the two Mo^{6+} centers. In this configuration, each Mo^{6+} ion is shifted along the C_3 rotational axis of the FSBO anion toward its respective fac-oriented terminal oxide ligands. This out-of-center movement mimics the primary distortion that has been observed in the related $[MoO_3F_3]^{3-}$ anion and results in terminal Mo═O bond lengths that are close to those in $[MoO_3F_3]^{3-}$ as well as tthose in other compounds such as $(Me_4N)_3(Mo_4O_{12}F_3)\cdot 0.8H_2O$.

The two poorly screened Mo^{6+} centers in $[Mo_2O_6F_3]^{3-}$ are separated by a distance of 3.17 Å, and as a result, the bridging metal−ligand−metal interactions are required to be long. Theoretical studies by Hoffmann and co-workers which relate the overall shape of an FSBO anion to its bonding and electronic structure show that, in a molecular anion such as $[Mo_2O_6F_3]^{3-}$, with π-donating ligands in both bridging and terminal positions, a large M−M separation tends to decrease the covalent metal−ligand overlap in the bridging sites. At the same time, calculated bond overlap populations show that there is a large π component to the terminal Mo═O bonds. When all three of the electronegative fluoride ligands in $[Mo_2O_6F_3]^{3-}$ are placed in bridging positions, they occupy less covalent bonding environments and allow the oxides to participate in strong π bonds with the metal centers. This specific ligand configuration also eliminates all destabilizing trans O−Mo−O interactions.

Acknowledgment. We thank Dr. Frederick P. Arnold for valuable discussions. We also gratefully acknowledge support from the National Science Foundation, (Solid State Chemistry Award Nos. DMR-9727516 and DMR-0312136) and made use of the Central Facilities supported by the MRSEC program of the National Science Foundation (DMR-0076097) at the Materials Research Center of Northwestern University.

Supporting Information Available: One X-ray crystallographic file in CIF format including crystallographic details, atomic coordinates, anisotropic thermal parameters, and interatomic distances and angles, one IR spectrum of $[Cu(3\text{-apy})_4]_3(Mo_2O_6F_3)_2$, and a text document containing GAMESS-US input parameters, input coordinates, final absolute energies, and converged atomic coordinates. This material is available free of charge via the Internet at http://pubs.acs.org.

IC0502877